Journal of Solid Mechanics Vol. 9, No. 1 (2017) pp. 198-212

The Effects of Carbon Nanotube Orientation and Aggregation on Static Behavior of Functionally Graded Nanocomposite Cylinders

R. Moradi-Dastjerdi [1], G. Payganeh [1,*], M. Tajdari [2]

[1] *School of Mechanical Engineering, Shahid Rajaee Teacher Training University (SRTTU), Tehran, Iran*
[2] *Department of Mechanical Engineering, Arak Branch, Islamic Azad University, Arak, Iran*

Received 10 January 2017; accepted 7 March 2017

ABSTRACT

In this paper, the effects of carbon nanotube (CNT) orientation and aggregation on the static behavior of functionally graded nanocomposite cylinders reinforced by CNTs are investigated based on a mesh-free method. The used nanocomposites are made of the straight CNTs that are embedded in an isotropic polymer as matrix. The straight CNTs are oriented, randomly or aligned or local aggregated into some clusters. The volume fractions of the CNTs and clusters are assumed variable along the thickness, so mechanical properties of the carbon nanotube reinforced composite cylinders are variable and are estimated based on the Eshelby–Mori–Tanaka approach. The obtained mechanical properties are verified by experimental and theoretical results that are reported in literatures. In the mesh-free analysis, moving least squares (MLSs) shape functions are used for approximation of displacement field in the weak form of equilibrium equation. Also, the effects of CNT distribution type and cylinder thickness are investigated on the stress distribution and displacement field of these cylinders.

Keywords : Nanocomposite cylinder; Aggregation; Mori–Tanaka; Static behavior; Functionally graded; Mesh-Free.

1 INTRODUCTION

AFTER the carbon nanotubes (CNTs) discovered by Iijima [1], the use of CNTs has been attracted widely in polymer/ CNT composites [2]. A high aspect ratio of CNT and extraordinary mechanical properties (strength and flexibility) provide the ultimate reinforcement for the next generation of extremely lightweight but highly elastic and very strong advanced composite materials. Most studies on nanocomposite reinforced by CNT have focused on their material properties [3-7]. Some investigations have also shown that the addition of small amount of CNT in the matrix can considerably improve the mechanical, electrical and thermal properties of polymeric composites [7-10]. Han and Elliott [6] determined the elastic modulus of composite structures under CNTs reinforcement by molecular dynamic simulation and investigated the effect of volume fraction of single-walled carbon nanotubes (SWCNTs) on mechanical properties of nanocomposites.

One of the common features of CNT morphology is the formation of aggregation in the matrix. Aggregation into bundles or ropes limits the overall effectiveness of nanotubes at improving the mechanical properties of the nanocomposite. The large aspect ratio (usually >1000), nanotube volume fraction, low bending rigidity of CNTs and interfacial bonding in the inter-phase region between embedded CNT and its surrounding polymer lead to their

*Corresponding author. Tel.: +98 21 22970052; Fax:+98 21 22970033.
E-mail address: g.payganeh@srttu.edu (G. Payganeh).

aggregation. Local aggregation of the nanotube in the polymer host is reduced significantly by functionalizing the nanotubes, thereby increasing the compatibility with the polymer. Montazeri et al. [11] showed the influence of aggregation of nanotube using the modified Halpin-Tsi model. Also they indicated that above 1.5 wt.%, nanotubes agglomerate causing a reduction in Young's modulus values. Thus, it is important to determine the effect of the distribution and arrangement of CNTs on the effective properties of carbon nanotube reinforced composite (CNTRC). The Mori–Tanaka (MT) model is one of the best known analytical approaches to determine the effective material constants of composite materials. Barai and Weng [12] developed a two-scale micromechanical model to analyze the effect of CNT aggregation and interface condition on the plastic strength of CNT/matrix inclusions, and the small scale addressed the property of the clustered inclusions. Yang et al. [13] used the Mori-Tanaka approach to show the effect of CNT aggregation in the composite. They illustrated the degree of CNT aggregation dramatically influences the effective properties of the CNT/SMP composites. Jam et al. [14] obtained effective elastic properties for CNTRC through a variety of micromechanics techniques. They used the elasticity theory to characterize the elastic properties of CNTRC based on Eshelby–Mori–Tanaka approach for an equivalent fiber. In this study the variations of mechanical properties with tube radius, interphase thickness, and degree of aggregation were investigated and it is shown that the presence of aggregates has stronger impact than the interphase thickness on the effective modulus of the composite.

Some researchers had also investigated on the mechanical behavior of nanostructures such as carbon nanotubes, nanorods and nanoplates. Farajpour et al. [15] studied the buckling behavior of nanoscale circular plates under uniform radial compression. They are considered the small-scale effect is taken into consideration and derived the governing equations of the circular single-layered graphene sheets (SLGS) by using of nonlocal elasticity theory. Janghorban and Zare [16] presented free vibration analysis of functionally graded carbon nanotube with variable thickness based on the Timoshenko beam theory. They also adopted the differential quadrature method (DQM) to solve the equations of motion. Malekzadeh and Farajpour [17] studied the axisymmetric free and forced vibrations of circular single- and double-layered nanoplates under initial in-plane radial stresses and embedded in an elastic medium. They used Eringen theory to derive the governing equations and Galerkin's method to solve the resulting equation for vibration frequencies and dynamic response. Axial vibration analysis of a tapered nanorod based on nonlocal elasticity theory and DQM is presented by Danesh et al. [18]. Also, the in-plane and out-of-plane nonlinear size-dependent dynamics of a microplate resting on an elastic foundation, constrained by distributed rotational springs at boundaries is examined by Gholipour et al. [19]. Golmakani and Rezatalab [20] studied on non-uniform biaxial buckling analysis of orthotropic single-layered graphene sheet embedded in a Pasternak elastic medium by using the nonlocal Mindlin plate theory. The nonlocal differential constitutive relations of Eringen and DQM are used in this study.

New class of materials known as functionally graded materials (FGMs) are special composites in which volume fractions of constituent materials vary uniformly and continuously along a certain direction(s). Therefore FGMs have a non uniform microstructure and a continuously variable macrostructure. By using the concept of FGM, Shen [21] suggested that the interfacial bonding strength can be improved through the use of a graded distribution of CNTs in the matrix and investigated postbuckling of functionally graded nanocomposite cylindrical shells reinforced by SWCNTs subjected to axial compression in thermal environment and showed that the linear functionally graded reinforcements can increase the buckling load. Tsai et al. [22] used the Mori-Tanaka approach to show the effect of inclusion waviness and its distribution on the effective composite stiffness. They considered different waviness conditions: uniform waviness with variable inclusion orientation or aspect ratio, uniform aspect ratio and variable waviness and they understood that the inclusion waviness have a great effect on the tensile moduli and shear modulus for unidirectional composites. Sobhani Aragh et al. [23] presented vibrational behavior of continuously graded CNT–reinforced cylindrical panels based on the Eshelby–Mori–Tanaka approach. They used the 2D Generalized Differential Quadrature Method (GDQM) to discretize the governing equations and to implement the boundary conditions. Also, Pourasghar et al. [24] presented free vibrations analysis of four-parameter continuously graded nanocomposite cylindrical panels reinforced by randomly oriented straight and local aggregation CNTs based on three-dimensional theory of elasticity. They estimated material properties of continuously graded CNTRCs through the Eshelby–Mori–Tanaka approach. In the other work, free vibration analysis of FG nanocomposite sandwich plates reinforced by randomly oriented CNT is investigated by Moradi-Dastjerdi et al. [25]. They used a refined shear deformation plate theory and Eshelby–Mori–Tanaka approach in their work.

For static analysis of the cylinders, a mesh-free method is used; MLS shape functions are used for approximation of displacement field in the weak form of equilibrium equation. But MLS shape function does not satisfied Kronecker delta property so in proposed mesh-free method transformation method is applied for deriving the displacement field. This mesh-free method is used for static, free vibration, dynamic and stress wave propagation analysis of FGM cylinders [26-29]. After these works, Moradi-Dastjerdi et al. [30-31] static and dynamic analysis of

FG-nanocomposite cylinders reinforced by straight SWCNTs carried out by the same mesh-free method that is used in this paper. Also, axisymmetric natural frequencies of FG-nanocomposite cylinders reinforced by CNTs are oriented, aligned or randomly or locally aggregated into some clusters are investigated by Moradi-Dastjerdi et al. [32]. They used the same mesh-free method and Eshelby–Mori–Tanaka approach in their study and showed these methods have very high accuracy for these problems.

In this study, static behaviors of nanocomposite cylinders reinforced by straight SWCNTs are investigated by the mentioned mesh-free method. These straight CNTs are oriented aligned or randomly or local aggregated in to some clusters, while in Ref. [30] the CNTs have been long, straight and along the axial axes of cylinder and without any clusters of CNT. So, the material properties of nanocomposite are estimated too much. Also, the volume fractions of the CNTs and clusters are assumed to be functionally graded in the radial direction. Several micromechanical models have been proposed to explain the mechanical properties of the nanocomposites. Most of these models assume a homogeneous dispersion of the nanotubes in the matrix. At first effects of orientation and aggregation of straight CNTs are investigated on the effective mechanical properties of nanocomposite based on Eshelbi-Mori-Tanaka approach. Then these effects and effects of cylinder thickness and kind of CNTs distribution are investigated on the radial displacement, hoop and radial stresses of CNTRC cylinders.

2 GOVERNING EQUATIONS

The weak form of equilibrium equation is expressed by the following relation [31]:

$$\int_{\Omega} \sigma.\delta(\varepsilon)dv - \int_{\Gamma} F.\delta u ds = 0 \tag{1}$$

In the above relation, σ, ε, F and u are stress, strain, surface traction, displacement vectors, respectively. Γ is a part of boundary of domain Ω on which traction F is applied. For axisymmetric problems stress and strain vectors are as follows:

$$\sigma = [\sigma_r, \sigma_\theta, \sigma_z, \sigma_{rz}]^T \quad , \quad \varepsilon = [\varepsilon_r, \varepsilon_\theta, \varepsilon_z, \varepsilon_{rz}]^T \tag{2}$$

Stress vector is expressed in terms of strain vector by means of Hook's law:

$$\sigma = D\varepsilon \tag{3}$$

Matrix D was defined in [29] for an isotropic cylinder and in [31] for an orthotropic one.

3 MESH-FREE NUMERICAL ANALYSIS

In these analyses, moving least square (MLS) shape functions introduced by Lancaster and Salkauskas [33] is used for approximation of displacement vector in the weak form of motion equation. Displacement vector u can be approximated by MLS shape functions as follows:

$$u = [u_r, u_z]^T = \Phi \hat{u} \tag{4}$$

where $\hat{u}$ and Φ are virtual nodal values vector and shape functions matrix respectively.

$$\hat{u} = [(\hat{u}_r)_1, (\hat{u}_z)_1, ...(\hat{u}_r)_n, (\hat{u}_z)_n]^T \tag{5}$$

And

$$\Phi = \begin{bmatrix} \Phi_1 & 0 & \Phi_2 & 0 & . & . & . & . & \Phi_n & 0 \\ 0 & \Phi_1 & 0 & \Phi_2 & . & . & . & . & 0 & \Phi_n \end{bmatrix} \tag{6}$$

By using (4) for approximation of displacement vector, strain vector can be expressed in terms of virtual nodal values:

$$\varepsilon = B\hat{u} \tag{7}$$

where, matrix B was defined in the Ref. [31] and by Substitution of (3), (4) and (7) in (1) leads to:

$$K\hat{u} = f \tag{8}$$

where

$$k = \int_{\Omega} B^T DB\, dv \qquad f = \int_{\Gamma} \Phi^T F ds \tag{9}$$

or numerical integration, problem domain is discretized to a set of background cells with gauss points inside each cell. Then global stiffness matrix k is obtained numerically by sweeping all gauss points. Finally, the relation between nodal displacement vector U and virtual displacement vector $\hat{u}$ is as follow:

$$U = T\hat{u} \tag{10}$$

where, T is transformation matrix and is defined in the Ref. [31].

4 MATERIAL PROPERTIES IN FG-CNT REINFORCED COMPOSITE

Consider a CNTRC is made from a mixture of SWCNT (that is aligned or randomly oriented or aggregated) and matrix which is assumed to be isotropic. Many studies have been published each with a different focus on mechanical properties of polymer nanotube composites. However, the common theme seems to have been enhancement of Young's modulus. In this section, the effective mechanical properties of this composite that the straight CNTs are oriented aligned or randomly or local aggregated into some clusters are obtained based on the Eshelby–Mori–Tanaka approach.

4.1 Composites reinforced with aligned, straight CNTs

The Mori–Tanaka method was used to predict the elastic stiffness properties of the CNT reinforced composite. For this current method, the complete elastic stiffness tensor for the composite is given by [34].

$$C = C_m + f_r \left\langle (C_r - C_m) A_r \right\rangle \left(f_m I + f_r \left\langle A_r \right\rangle \right)^{-1} \tag{11}$$

where f_r and f_m are the fiber and matrix volume fractions, respectively, C_m is the stiffness tensor of the matrix material, C_r is the stiffness tensor of the fiber, I is the forth order identity tensor and A_r is the dilute strain-concentration tensor of the r th phase for the fiber which is given as:

$$A_r = \left[I + S (C_m)^{-1} (C_r - C_m) \right]^{-1} \tag{12}$$

The tensor S is Eshelby's tensor, as given by Eshelby [35] and Mura [36]. The terms enclosed with angle brackets in (11) represent the average value of the term over all orientations defined by transformation from the

local fiber coordinates $(o-x'_1x'_2x'_3)$ to the global coordinates $(o-x_1x_2x_3)$ (Fig. 1). Assume axis x_2 being the direction along the aligned nanotube. The elastic properties of the nanocomposite are determined from the average strain obtained in the representative volume element. The matrix is assumed to be elastic and isotropic, with Young's modulus E_m and Poisson's ratio v_m. Each straight CNT is modeled as along fiber with transversely isotropic elastic properties and have a stiffness matrix given by (11). Therefore, the composite is also transversely isotropic, with five independent elastic constants. The substitution of non-vanishing components of the Eshelby tensor *S* for a straight, long fiber along the x_2-direction [34] in (12) gives the dilute mechanical strain concentration tensor. Then the substitution of (12) into (11) gives the tensor of effective elastic moduli of the composite reinforced by aligned, straight CNTs. In particular, the Hill's elastic moduli are found as [34].

$$k=\frac{E_m\left\{E_m f_m+2k_r(1+v_m)\left[1+f_r(1-2v_m)\right]\right\}}{2(1+v_m)\left[E_m(1+f_r-2v_m)+2f_m k_r(1-v_m-2v_m^2)\right]} \tag{13}$$

$$l=\frac{E_m\left\{v_m f_m+\left[E_m+2k_r(1+v_m)\right]+2f_r k_r(1-v_m^2)\right\}}{(1+v_m)\left[E_m(1+f_r-2v_m)+2f_m k_r(1-v_m-2v_m^2)\right]} \tag{14}$$

$$n=\frac{E_m^2 f_m(1+f_r-f_m v_m)+2f_m f_r(k_r n_r-l_r^2)(1+v_m)^2(1-2v_m)}{(1+v_m)\left[E_m(1+f_r-2v_m)+2f_m k_r(1-v_m-2v_m^2)\right]}+ \\ \frac{E_m\left[2f_m^2 k_r(1-v_m)+f_r n_r(1+f_r-2v_m)-4f_m l_r v_m\right]}{E_m(1+f_r-2v_m)+2f_m k_r(1-v_m-2v_m^2)} \tag{15}$$

$$p=\frac{E_m\left[E_m f_m+2p_r(1+v_m)(1+f_r)\right]}{2(1+v_m)\left\{E_m\left[f_m+4f_r(1-v_m)+2f_m m_r(3-v_m-4v_m^2)\right]\right\}} \tag{16}$$

$$m=\frac{E_m\left[E_m f_m+2m_r(1+v_m)(3+f_r-4v_m)\right]}{2(1+v_m)\left\{E_m\left[f_m+4f_r(1-v_m)+2f_m m_r(3-v_m-4v_m^2)\right]\right\}} \tag{17}$$

where *k*, *l*, *m*, *n* and *p* are its plane-strain bulk modulus normal to the fiber direction, cross modulus, transverse shear modulus, axial modulus and axial shear modulus respectively. k_r, l_r, m_r, n_r and p_r are the Hill's elastic moduli for the reinforcing phase (CNTs). Therefore the axial and transverse Young's modulus of the composite can be calculated from the Hill's elastic modulus.

$$E_1=n-\frac{l^2}{k} \tag{18}$$

$$E_2=\frac{4m(kn-l^2)}{kn-l^2+mn} \tag{19}$$

f_r and f_m are the volume fractions for carbon nanotube and matrix and are related by

$$f_r+f_m=1 \tag{20}$$

As mentioned before, the CNTs are transversely isotropic and have a stiffness matrix given below (Hill's elastic moduli)

$$C_r = \begin{bmatrix} n_r & l_r & l_r & 0 & 0 & 0 \\ l_r & k_r + m_r & k_r - m_r & 0 & 0 & 0 \\ l_r & k_r - m_r & k_r + m_r & 0 & 0 & 0 \\ 0 & 0 & 0 & p_r & 0 & 0 \\ 0 & 0 & 0 & 0 & m_r & 0 \\ 0 & 0 & 0 & 0 & 0 & p_r \end{bmatrix} \tag{21}$$

$$C_r = \begin{bmatrix} \frac{1}{E_L} & -\frac{v_{TL}}{E_T} & -\frac{v_{ZL}}{E_Z} & 0 & 0 & 0 \\ -\frac{v_{LT}}{E_L} & \frac{1}{E_T} & -\frac{v_{ZT}}{E_Z} & 0 & 0 & 0 \\ -\frac{v_{LZ}}{E_L} & -\frac{v_{TZ}}{E_T} & \frac{1}{E_Z} & 0 & 0 & 0 \\ 0 & 0 & 0 & \frac{1}{G_{TZ}} & 0 & 0 \\ 0 & 0 & 0 & 0 & \frac{1}{G_{ZL}} & 0 \\ 0 & 0 & 0 & 0 & 0 & \frac{1}{G_{LT}} \end{bmatrix} \tag{22}$$

where $E_L, E_T, E_Z, G_{TZ}, G_{ZL}, G_{LT}, v_{LT}, v_{LT}$ are material properties of the CNT reinforced composite which can be determined from the inverse of the rule of mixture.

4.2 Effect of CNT aggregation on the properties of the composite

The CNTs were arranged within the matrix in such manner so as to introduce clustering. It has been observed that, due to large aspect ratio (usually >1000), low bending rigidity of CNTs and Van der Waals forces, CNTs have a tendency to bundle or cluster together making it quite difficult to produce fully-dispersed CNT reinforced composites. The effect of nanotube aggregation on the elastic properties of randomly oriented CNTRC is presented in this section. Shi et al. [34] derived a two parameter micromechanics model to determine the effect of nanotube agglomeration on the elastic properties of randomly oriented CNTRC (Fig. 2). It is assumed that a number of CNTs are uniformly distributed throughout the matrix and that other CNTs appear in cluster form because of aggregation, as shown in Fig. 2. The total volume of the CNTs in the representative volume element (RVE), denoted by V_r, can be divided into the following two parts:

$$V_r = V_r^{cluster} + V_r^m \tag{23}$$

where $V_r^{cluster}$ denote the volumes of CNTs inside a cluster, and V_r^m is the volume of CNTs in the matrix and outside the clusters. The two parameters used to describe the aggregation are defined as:

$$\mu = \frac{V_{cluster}}{V}, \quad \eta = \frac{V_r^{cluster}}{V_r} \qquad 0 \le \eta, \mu \le 1 \tag{24}$$

where V is volume of RVE, $V_{cluster}$ is volume of clusters in the RVE. μ is volume fraction of clusters with respect to the total volume V of the RVE, η is volume ratio of the CNTs inside the clusters over the total CNT inside the RVE. When $\mu = 1$, this means uniform distribution of nanotubes throughout the entire composite without aggregation, and with the decreasing in μ, the agglomeration degree of CNTs is more severe. When $\eta = 1$, all the nanotubes are located in the clusters. The case $\eta = \mu$ means that the volume fraction of CNTs inside the clusters is as same as that of CNTs outside the clusters so all CNTs are located randomly oriented same as Fig. 1.

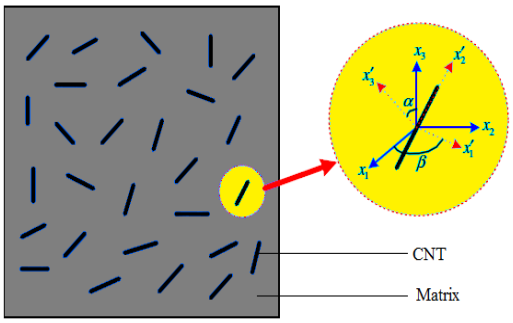

Fig.1
Representative volume element (RVE) with randomly oriented, straight CNTs.

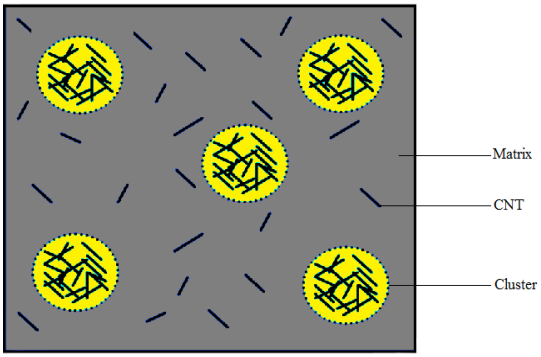

Fig.2
Representative Volume Element (RVE) With Eshelby cluster model of aggregation of CNTs.

Thus, we consider the CNT-reinforced composite as a system consisting of clusters of sphere shape embedded in a matrix. We may first estimate respectively the effective elastic stiffness of the clusters and the matrix, and then calculate the overall property of the whole composite system. The effective bulk modulus K_{in} and shear modulus G_{in} of the cluster can be calculated by [37], respectively:

$$K_{in} = K_m + \frac{f_r \eta(\delta_r - 3K_m \alpha_r)}{3(\mu - f_r \eta + f_r \eta \alpha_r)} \tag{25}$$

$$G_{in} = G_m + \frac{f_r \eta(\eta_r - 2G_m \beta_r)}{2(\mu - f_r \eta + f_r \eta \beta_r)} \tag{26}$$

And the effective bulk modulus K_{out} and shear modulus G_{out} of the matrix outside the cluster can be calculated by:

$$K_{out} = K_m + \frac{f_r (1-\eta)(\delta_r - 3K_m \alpha_r)}{3\left[1 - \mu - f_r (1-\eta) + f_r (1-\eta)\alpha_r\right]} \tag{27}$$

$$G_{out} = G_m + \frac{f_r (1-\eta)(\eta_r - 2G_m \beta_r)}{2\left[1 - \mu - f_r (1-\eta) + f_r (1-\eta)\beta_r\right]} \tag{28}$$

Finally, the effective bulk modulus K and the effective shear modulus G of the composite are derived from the Mori-Tanaka method as follows:

$$K = K_{out}\left[1+\frac{\mu\left(\frac{K_{in}}{K_{out}}-1\right)}{1+\alpha(1-\mu)\left(\frac{K_{in}}{K_{out}}-1\right)}\right] \tag{29}$$

$$G = G_{out}\left[1+\frac{\mu\left(\frac{G_{in}}{G_{out}}-1\right)}{1+\beta(1-\mu)\left(\frac{G_{in}}{G_{out}}-1\right)}\right] \tag{30}$$

with

$$G_{out} = \frac{(3K_{out}-2G_{out})}{2(3K_{out}+G_{out})} \tag{31}$$

$$\alpha = \frac{(1+v_{out})}{3(1-v_{out})} \tag{32}$$

$$\beta = \frac{2(4-5v_{out})}{15(1-v_{out})} \tag{33}$$

The effective Young's modulus E and Poisson's ratio υ of the composite can be calculated in the terms of K and G by:

$$E = \frac{9KG}{3K+G} \tag{34}$$

$$v = \frac{3K-2G}{6K+2G} \tag{35}$$

5 RESULTS AND DISCUSSIONS

In this section, at first the used mesh-free method and the calculation approach of the nanocomposite modulus are validated and then effects of various parameters on the static responses of CNTRC cylinders are investigated. The mesh-free results are compared with results of FEM. To compare the results of mesh-free and finite element (FE) analyses, the same nodes arrangements are used in these two types of analyses. For this reason, regular grid arrangements are used in all simulations although irregular grid arrangements can be used for mesh-free simulations easily. In this work for all FE simulations, rectangular four-node axisymmetric elements are used.

5.1 Validation of models

For validation of used mesh-free model, stress distributuion of an FGM cylinder is investigated. Consider an infinite length cylinder subjected to internal pressure (P_i , from inside to outside) and with ratio of inner radius to outer is equal to $r_i/r_0 = 0.5$ and variation of elasticity modulus is given by:

$$E = E_i \left(\frac{r}{r_i}\right)^n, \qquad n = \ln\left(\frac{E_o}{E_i}\right) / \ln\left(\frac{r_o}{r_i}\right) \tag{36}$$

where E_i and E_0 are elasticity modulus at inner and outer radius respectively. Also numerical values $E_i = 200$ and $E_0 = 360GPa$ are used. Variation of normalized values of radial and hoop stresses (σ/P_i) along the radial direction are shown in Fig. 3. As shown in this figure, results obtained from the mesh-free method are in good agreement with analytical solution introduced by Tutuncu and Temel [38] and results obtained from FEM.

After validation of the used mesh-free model, the Mori-Tanaka approach that is applied for calculation of the nanocomposite modulus is examined. This approach can examine the effects of orientation and aggregation of the CNTs in the matrix. These cases have a significant effect on the material properties of CNT nanocomposite. As mentioned before the parameters μ and η can be used to describe distribution of CNTs-reinforced composite where μ and η are indicators of the volume fractions of clusters and CNTs in the clusters respectively. Fig. 4 shows Young's modulus of a CNT-reinforced composite for various value of μ when $\eta = 1$ that compared with the experimental data [39]. This figure shows that, for fully dispersed randomly oriented CNTs, $\mu = 1$, Young's modulus has the biggest value. Young's modulus decrease by decreasing of volume fraction of CNTs and also by decreasing of μ when η is constant (increasing of the CNTs aggregation). It can be also seen that the experimental data and the aggregation state of $\eta = 1$ and $\mu = 0.4$ are nearly the same. These results are in agreement with an argument proposed by Barai and Weng [12] too.

In the following simulations, CNTRC cylinders are considered made of Poly (methyl- methacrylate, referred as PMMA) as matrix, with CNT as fibers. PMMA is an isotropic material with $E^m = 2.5GPa, \rho^m = 1150Kg/m^3$ and $v^m = 0.34$. The (10,10) SWCNTs are selected as reinforcements. The adopted material properties for SWCNT are: $E_1^{CN} = 5.6466TPa, E_2^{CN} = 7.0800TPa, G_{12}^{CN} = 1.9445TPa, \rho^{CN} = 1400Kg/m^3$ and $v^{CN} = 0.175$ [21].
In this state the effects of distributions and orientations of the CNTs on the Young's modulus of a CNTRC are examined. Fig. 5 shows Young's modulus of alignment, randomly oriented and local aggregated of CNTRCs for various values of volume fraction of the CNTs. This figure shows that alignment oriented of CNTs estimate very high value for effective Young's modulus despite Fig. 4 shows the experimental data has the same values with $\mu = 0.4$ and $\eta = 1$. It can be also seen that randomly oriented or fully dispersed, $\mu = \eta = 1$, nanotubes have more stiffness than other aggregated state, $\mu = 0.4, 0.7, 0.9$.

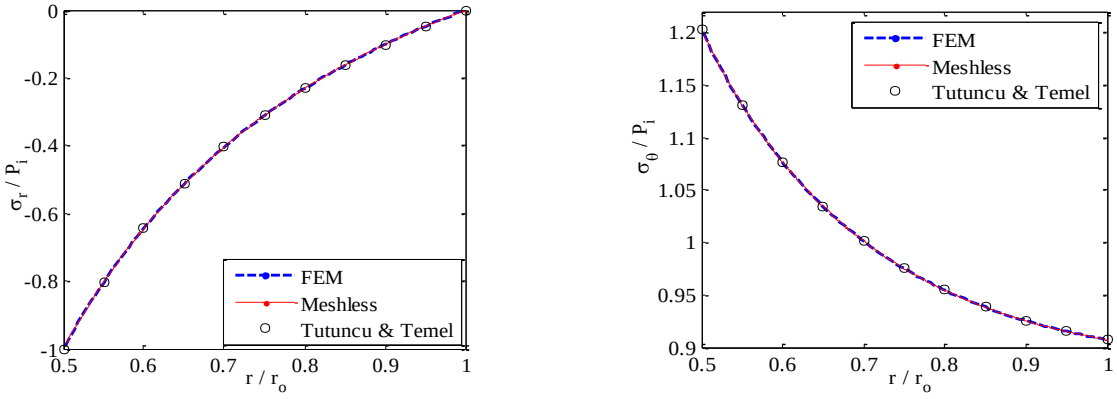

Fig.3
Variation of normalized values of a) radial stress b) hoop stress of FGM cylinder along the radial direction.

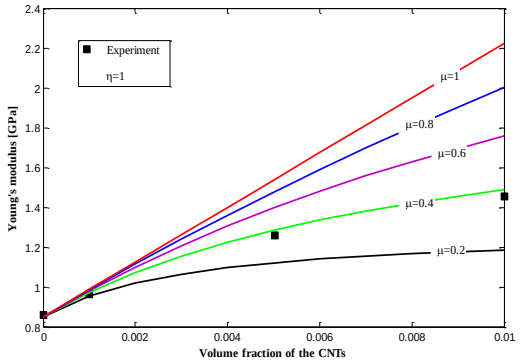

Fig.4
Comparison of the Young's modulus of CNT-reinforced composite at different degree of aggregation with the experimental data [39].

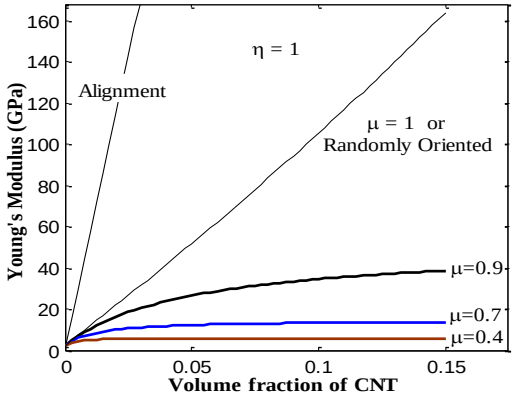

Fig.5
Comparison of the Young's modulus of CNT-reinforced composite at different degree of aggregation with the randomly oriented and aligned CNTs.

5.2 CNTRC Cylinders

After the validation of the applied methods, five different models of infinite length UD and FG-CNTRC cylinders are considered to investigate the effects of effective parameters on the static responses. In FG-CNTRC cylinder, volume fraction of nanotube, f_r, or volume of CNTs clusters, μ, vary along the radius according to:

$$p = p_i + \left(\frac{r - r_i}{r_o - r_i}\right)^n \left(p_o - p_i\right) \tag{37}$$

where, p_i and p_o are mechanical properties at inner and outer surfaces respectively and *n* is volume fraction power. Fig. 6 shows the variation of volume fraction of nanotube along the thickness of cylinders for different values of volume fraction powers, *n*. At first infinite length CNTRC cylinders are considered with the ratio of inner radius to outer, $r_i / r_0 = 0.5$, subjected to internal pressure, p_i, as first model. In these cylinders, CNTs oriented aligned and volume fraction of nanotube, f_r, varies from zero to 0.3 according to (38). These cylinders are compared with an UD-CNTRC cylinder with $f_r = 0.15$. This cylinder has the same CNT volume with FG-CNTRC with $n = 1$. So the effect of CNT distribution can be seen at the same CNT volume by comparing the results of these cylinders. The variations of radial displacement, hoop stress and radial stress of the cylinders of the first model were shown in Fig. 7. This figure reveals that increasing of the volume fraction power, *n*, increases the values of radial displacements and radial displacement of the FG-CNTRC with $n = 1$ is a little bigger than UD-CNTRC cylinder. Maximum values of the hoop stresses are near the inner surface and the values and variation of this stress was seen for UD cylinder and the minimum values was seen for FG-CNTRC cylinder with $n = 1$, so hoop stress is decreased by using FG types for CNT distribution. Lack of the CNT volume at inner surface and excess of this at outer surface lead to a severity decreasing and increasing in the hoop stresses of FG cylinders with $n = 0.1$ and $n = 10$ respectively. Also, the radial stress is uniformly varied from the value of internal pressure, p_i, on the inner surface to value of external

pressure (zero) on the outer surface. It can be seen, UD cylinder has the biggest values of radial stress and FG cylinders with $n=0.1$ has the smallest one.

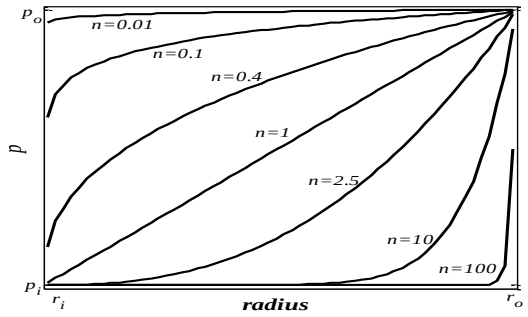

Fig.6
Variation of properties along the thickness of cylinders for different values of n according to (38).

Now, static behaviors of local aggregated CNTRC cylinders are investigated. In second model, FG and UD-CNTRC cylinders with ratio of radii, $r_i/r_0=0.5$, subjected to internal pressure, p_i, are considered like as first model. But in this model, nanotube aggregated in some clusters with aggregation state of $\mu=0.2$ and $\eta=1$ also in this model, volume fraction of nanotube, f_r, varies from zero to 0.3 too. Fig. 8 shows the variations of radial displacement, hoop stress and radial stress of these cylinders. This figure discloses radial deflection of FG cylinders with $n=10$ has biggest values in while three other cylinders have the near values of ones. It can be seen, displacements in the first model is bigger than the same values of cylinders of second model. In hoop stress variation, discloses that FG cylinder with $n=0.1$ has the same values with UD one; also these values for $n=10$ has an increasing around of mid radius. Moreover, the FG cylinder with $n=10$ has minimum values of the radial stress.

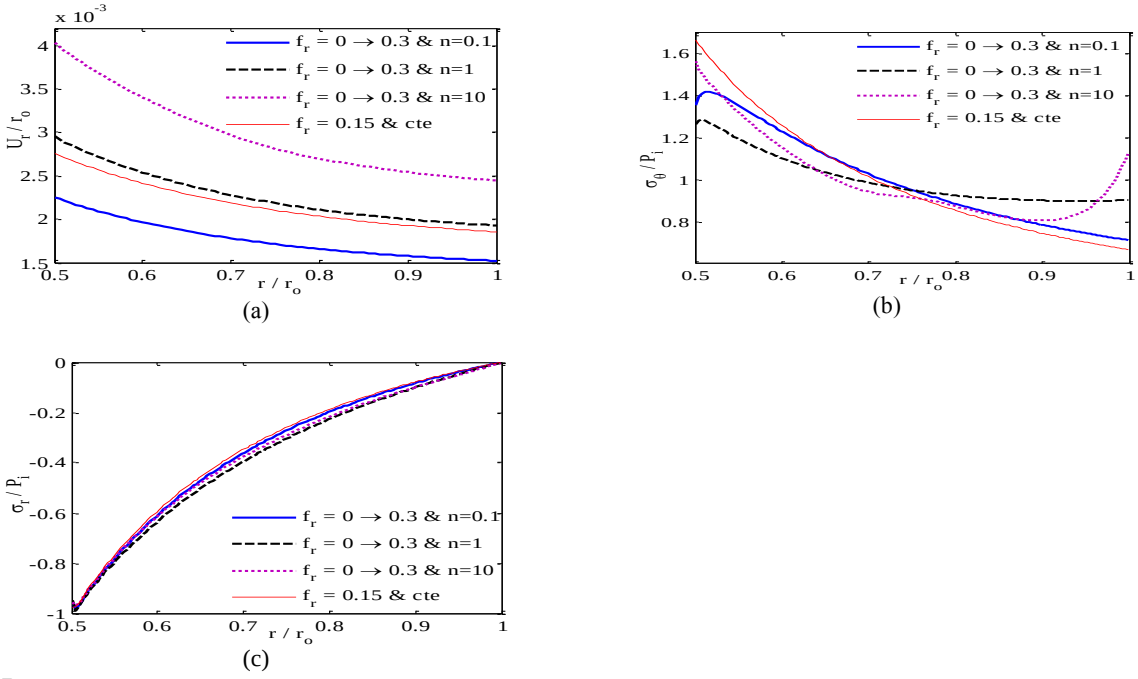

Fig.7
Variations of a) Radial displacement b) Hoop stress c) Radial stress of the CNTRC cylinders of the first model.

The cylinders of third model are same with second model cylinders but volume fraction of nanotube, f_r, varies from 0.3 in inner radius to zero at outer radius. Static responses of cylinders of this model were shown in Fig. 9. These figures show that displacement of FG cylinder with $n=0.1$ has the biggest values but displacement fields of all cylinders are near. In this model, UD and FG cylinders with $n=10$ have the same hoop stress distribution and the others cylinders have a drop in values of hoop stress at outer radius. This drop for cylinder with $n=0.1$ is

bigger than the other one. Also, the radial stress values of these cylinders are near together but the values of FG cylinder with $n = 0.1$ are bigger than the other ones.

In fourth model of CNTRC cylinders, effect of thickness can be investigable by decreasing the thickness of cylinder than similar ones in second. The cylinders of fourth model are similar to cylinders of second model but the ratio of radii is equal to, $r_i / r_0 = 0.8$, so the effect of thickness can be investigated. Fig. 10 shows the distributions of radial displacement, hoop stress and radial stress of the fourth model cylinders. By comparing between this figure and Fig. 8 reveals that decreasing of the thickness increases the values of displacements and hoop stresses about three times by the same trend with second model. In this model, decreasing and increasing of the hoop stress are more severe than second model and even maximum value of hoop stress for FG cylinder with $n = 10$ accrued around outer radius. Radial stresses change from the P_i on the inner surface to zero on the outer surface quicker than the correspond cylinders in second model.

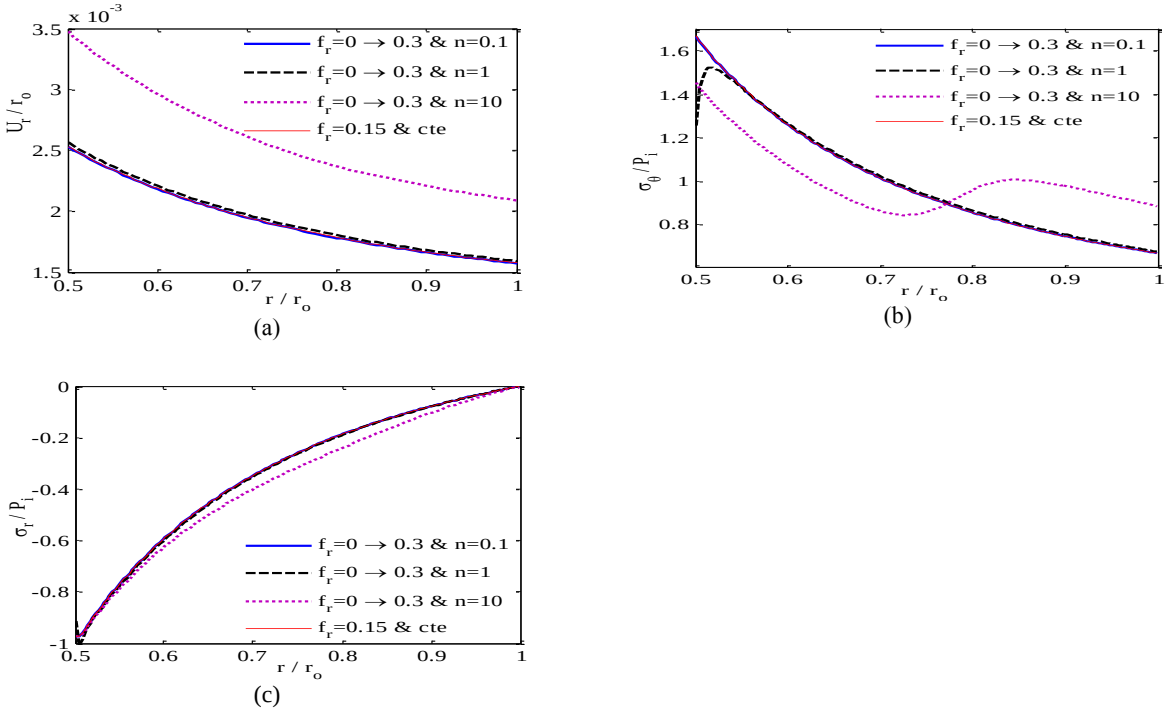

Fig.8
Variations of a) Radial displacement b) Hoop stress c) Radial stress of the CNTRC cylinders of the second model.

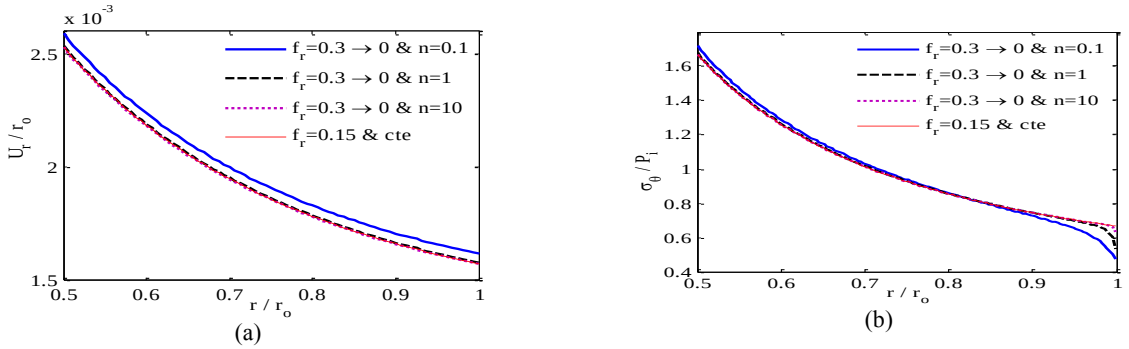

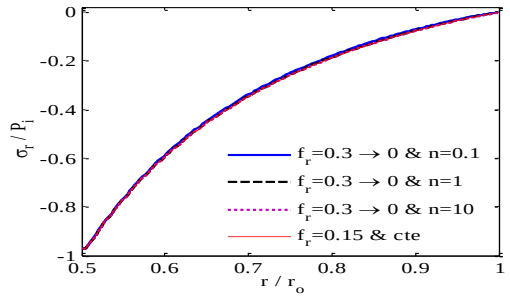

(c)

Fig.9
Variations of a) Radial displacement b) Hoop stress c) Radial stress of the CNTRC cylinders of the third model.

Finally, in the fifth model volume fraction of the clusters is assumed variable. These infinite length CNTRC cylinders are considered with the ratio radii, $r_i / r_0 = 0.5$, and subjected to internal pressure, P_i, too. In this model, CNT volume is constant and equal to, $f_r = 0.15$, with $\eta = 1$ but, μ is varied from 0.1 to 0.3 along radius according to (38). Static responses of this model are shown in Fig. 11. It can be seen that this result are so similar to results of first model with less values in displacement and hoop stress.

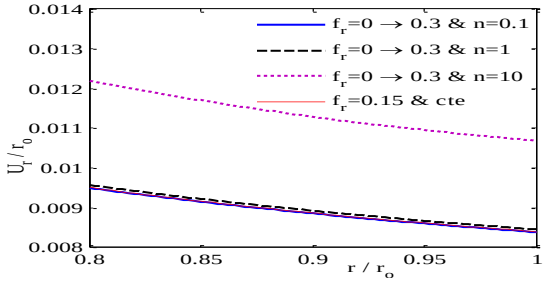

(a)

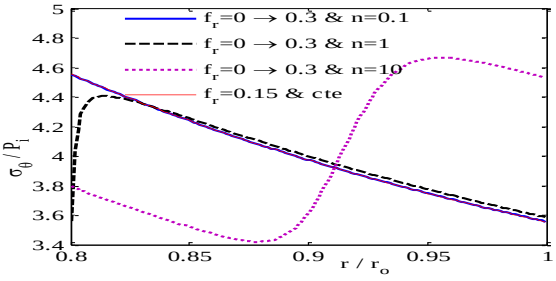

(b)

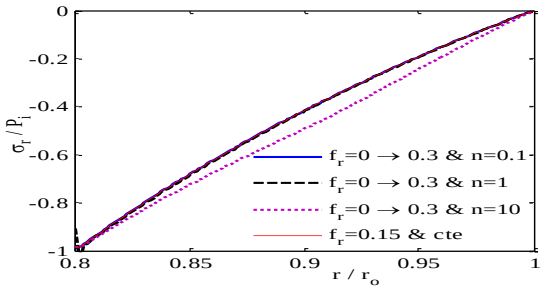

(c)

Fig.10
Variations of a) Radial displacement b) Hoop stress c) Radial stress of the CNTRC cylinders of the fourth model.

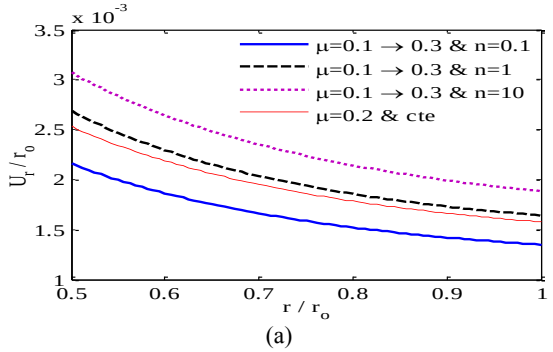

(a)

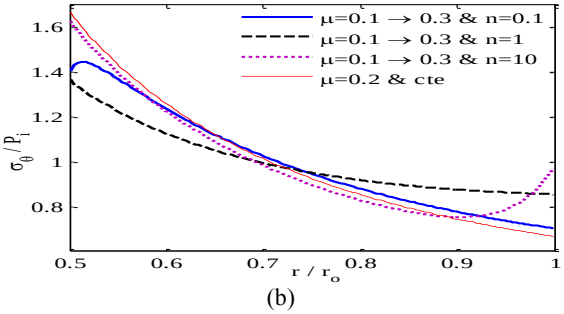

(b)

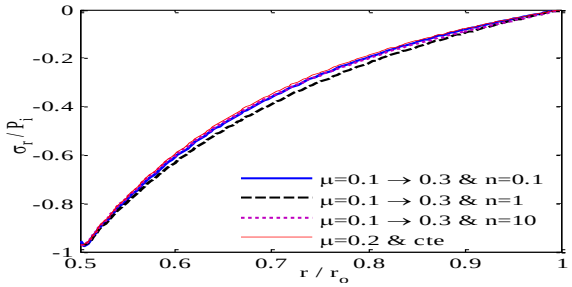

(c)

Fig.11
Variations of a) Radial displacement b) Hoop stress c) Radial stress of the CNTRC cylinders of the fifth model.

6 CONCLUSIONS

In this work by using a mesh-free method, effects of orientation and aggregation of CNTs on the static behaviors of functionally graded CNT- reinforced composite cylinders were analyzed. Volume fractions of the CNTs and clusters were assumed to be functionally graded along the thickness so that material properties of the CNTRC cylinders were variable and were estimated based on the Eshelby–Mori–Tanaka approach. It is observed that type of distributions, aggregation or even random orientations of CNTs have a significant effect on the effective stiffness and frequency parameter. The following results were obtained from this analysis:

- Nanocomposites that are reinforced by aligned CNTs have the biggest value of Young's modulus and nanocomposites with some clusters of CNTs have the smallest values of one.
- Decreasing of CNT volume fraction, increasing of the clusters volume, μ, or decreasing of the concentration of CNTs in clusters, η, decreases the value of Young's modulus.
- The power of CNT volume fraction, *n*, or CNT distribution kind has a great effect on the hoop stress field especially on the maximum hoop stress.
- Increasing in power of cluster or CNT volume fraction increase the values of radial displacements.
- Radial stress in cylinders of all models is varied uniformly from value of internal pressure to value of external pressure along the radius.
- Decreasing the thickness increases the values of displacements and hoop stresses with the same trend.

REFERENCES

[1] Iijima S., 1991, Helical microtubules of graphitic carbon, *Nature* **354**: 56-58.
[2] Wagner H.D., Lourie O., Feldman Y., Tenne R., 1997, Stress-induced fragmentation of multiwall carbon nanotubes in a polymer matrix, *Applied Physics Letters* **72**: 188-190.
[3] Griebel M., Hamaekers J., 2004, Molecular dynamic simulations of the elastic moduli of polymer-carbon nanotube composites, *Computer Methods in Applied Mechanics and Engineering* **193**: 1773-1788.
[4] Fidelus J.D., Wiesel E., Gojny F.H., Schulte K., Wagner H.D., 2005, Thermo-mechanical properties of randomly oriented carbon/epoxy nanocomposites, *Composite Part A* **36**: 1555-1561.
[5] Song Y.S., Youn J.R., 2006, Modeling of effective elastic properties for polymer based carbon nanotube composites, *Polymer* **47**: 1741-1748.
[6] Han Y., Elliott J., 2007, Molecular dynamics simulations of the elastic properties of polymer/carbon nanotube composites, *Computational Materials Science* **39**: 315-323.
[7] Zhu R., Pan E., Roy A.K., 2007, Molecular dynamics study of the stress–strain behavior of carbon-nanotube reinforced Epon 862 composites, *Materials Science and Engineering A* **447**: 51-57.
[8] Manchado M.A.L., Valentini L., Biagiotti J., Kenny J.M., 2005, Thermal and mechanical properties of single-walled carbon nanotubes-polypropylene composites prepared by melt processing, *Carbon* **43**: 1499-1505.
[9] Qian D., Dickey E.C., Andrews R., Rantell T., 2000, Load transfer and deformation mechanisms in carbon nanotube–polystyrene composites, *Applied Physics Letters* **76**: 2868-2870.
[10] Mokashi V.V., Qian D., Liu Y.J., 2007, A study on the tensile response and fracture in carbon nanotube-based composites using molecular mechanics, *Composites Science and Technology* **67**: 530-540.

[11] Montazeri A., Javadpour J., Khavandi A., Tcharkhtchi A., Mohajeri A., 2010, Mechanical properties of multi-walled carbon nanotube/epoxy composites, *Material & Design* **31**: 4202-4208.
[12] Barai P., Weng G.J., 2011, A theory of plasticity for carbon nanotube reinforced composite, *International Journal of Plastic* **27**: 539-559.
[13] Yang Q.S., He X.Q., Liu X., Leng F.F., Mai Y.W., 2012, The effective properties and local aggregation effect of CNT/SMP composites, *Composites Part B* **43**: 33-38.
[14] Jam J.E., Pourasghar A., kamarian S., Maleki Sh., 2013, Characterizing elastic properties of carbon nanotube-based composites by using an equivalent fiber, *Polymer Composites* **34**: 241-251.
[15] Farajpour A., Mohammadi M., Shahidi A.R., Mahzoon, M., 2011, Axisymmetric buckling of the circular graphene sheets with the nonlocal continuum plate model, *Physica E: Low-dimensional Systems and Nanostructures* **43**: 1820-1825.
[16] Jonghorban M., Zare A., 2011, Free vibration analysis of functionally graded carbon nanotubes with variable thickness by differential quadrature method, *Physica E: Low-dimensional Systems and Nanostructures* **43**:1602-1904.
[17] Malekzadeh P., Farajpour A., 2012, Axisymmetric free and forced vibrations of initially stressed circular nanoplates embedded in an elastic medium, *Acta Mechanica* **223**: 2311-2330.
[18] Danesh M., Farajpour A., Mohammadi M., 2012, Axial vibration analysis of a tapered nanorod based on nonlocal elasticity theory and differential quadrature method, *Mechanics Research Communications* **39**: 23-27.
[19] Gholipour A., Farokhi H., Ghayesh M.H., 2015, In-plane and out-of-plane nonlinear size-dependent dynamics of microplates, *Nonlinear Dynamics* **79**: 1771-1785.
[20] Golmakani M.E., Rezatalab J., 2015, Nonuniform biaxial buckling of orthotropic nanoplates embedded in an elastic medium based on nonlocal Mindlin plate theory, *Composite Structures* **119**: 238-250.
[21] Shen H.S., 2011, Postbuckling of nanotube-reinforced composite cylindrical shells in thermal environments, Part I: Axially-loaded shells, *Composite Structures* **93**: 2096-2108.
[22] Tsai C., Zhang C., Jack D.A., Liang R., Wang B., 2011, The effect of inclusion waviness and waviness distribution on elastic properties of fiber-reinforced composites, *Composites Part B* **42**: 62-70.
[23] Sobhani Aragh B., Nasrollah Barati A.H., Hedayati H., 2012, Eshelby–Mori–Tanaka approach for vibrational behavior of continuously graded carbon nanotube–reinforced cylindrical panels, *Composites Part B* **43**: 1943-1954.
[24] Pourasghar A., Yas M.H., Kamarian S., 2013, Local aggregation effect of CNT on the vibrational behavior of four-parameter continuous grading nanotube-reinforced cylindrical panels, *Polymer Composites* **34**: 707-721.
[25] Moradi-Dastjerdi R., Payganeh Gh., Malek-Mohammadi H., 2015, Free vibration analyses of functionally graded CNT reinforced nanocomposite sandwich plates resting on elastic foundation, *Journal of Solid Mechanics* **7**:158-172.
[26] Foroutan M., Moradi-Dastjerdi R., Sotoodeh-Bahreini R., 2012, Static analysis of FGM cylinders by a mesh-free method, *Steel and Composite Structures* **12**: 1-11.
[27] Mollarazi H.R., Foroutan M., Moradi-Dastjerdi R., 2011, Analysis of free vibration of functionally graded material (FGM) cylinders by a meshless method, *Journal of Composite Materials* **46**: 507-515.
[28] Moradi-Dastjerdi R., Foroutan M., 2014, Free vibration analysis of orthotropic FGM cylinders by a mesh-free method, *Journal of Solid Mechanics* **6**: 70-81.
[29] Foroutan M., Moradi-Dastjerdi R., 2011, Dynamic analysis of functionally graded material cylinders under an impact load by a mesh-free method, *Acta Mechanica* **219**: 281-290.
[30] Moradi-Dastjerdi R., Foroutan M., Pourasghar A., Sotoudeh-Bahreini R., 2013, Static analysis of functionally graded carbon nanotube-reinforced composite cylinders by a mesh-free method, *Journal of Reinforced Plastics and Composites* **32**: 593-601.
[31] Moradi-Dastjerdi R., Foroutan M., Pourasghar A., 2013, Dynamic analysis of functionally graded nanocomposite cylinders reinforced by carbon nanotube by a mesh-free method, *Material & Design* **44**: 256-266.
[32] Moradi-Dastjerdi R., Pourasghar A., Foroutan M., 2013, The effects of carbon nanotube orientation and aggregation on vibrational behavior of functionally graded nanocomposite cylinders by a mesh-free method, *Acta Mechanica* **224**: 2817-2832.
[33] Lancaster P., Salkauskas K., 1981, Surface generated by moving least squares methods, *Mathematics of Computation* **37**: 141-158.
[34] Shi D.L., Feng X.Q., Yonggang Y.H., Hwang K.C., Gao H., 2004, The effect of nanotube waviness and agglomeration on the elasticproperty of carbon nanotube reinforced composites, *Journal of Engineering Materials and Technology* **126**: 250-257.
[35] Eshelby J.D., 1957, The determination of the elastic field of an ellipsoidal inclusion, and related problems, *Proceedings of the Royal Society of London Series A* **241**: 376-396.
[36] Mura T., 1982, *Micromechanics of Defects in Solids*, The Hague, Martinus Nijhoff Pub.
[37] Prylutskyy Y.I., Durov S.S., Ogloblya O.V., Buzaneva E.V., Scharff P., 2000, Molecular dynamics simulation of mechanical, vibrational and electronic properties of carbon nanotubes, *Computational Materials Science* **17**: 352-355.
[38] Tutuncu N., Temel B., 2009, A novel approach to stress analysis of pressurized FGM cylinders, disks and spheres, *Journal of Composite Structures* **91**: 385-390.
[39] Odegard G.M., Gates T.S., Wise K.E., Park C., Siochi E.J., 2003, Constitutive modeling of nanotube-reinforced polymer composites, *Composites Science and Technology* **63**: 1671-1687.